



Molecularly imprinted photopolymers combined with smartphone-based optical sensing for selective detection of bisphenol A in foods

Dounia Elfadil¹ · Aziz Amine¹

Received: 20 December 2023 / Revised: 13 February 2024 / Accepted: 19 February 2024 / Published online: 11 March 2024
© The Author(s), under exclusive licence to Springer-Verlag GmbH, DE part of Springer Nature 2024

Abstract

Bisphenol A (BPA), known for its endocrine-disrupting properties and potential to leach into food products, has led to significant food safety concerns. Therefore, the development of sensitive and selective BPA rapid detection methods is crucial. In this study, molecularly imprinted solid-phase extraction coupled to a colorimetric method was adopted for the smartphone-based determination of BPA. The molecularly imprinted polymer (MIP) was prepared via photopolymerization and used as a selective adsorbent material for SPE columns. The solid-phase extraction (SPE) columns with multiple cycles significantly reduced the extraction time to only 30 min. The developed method demonstrates useful sensitivity for BPA (LOD = 30 ppb). Furthermore, BPA migration from plastic packaging was evaluated under different storage conditions, revealing that microwave treatment for 5 min led to BPA release from polycarbonate packaging in juice and basic solutions. The MIP selective extraction/clean-up and smartphone-based optical sensor were successfully applied to BPA standard solutions and complex food samples (e.g., juice and tap water), resulting in reproducible and selective BPA determination (RSD ≤ 6%, $n = 3$). This rapid and cost-effective method of producing MIPs for BPA offers a promising solution for fast and low-cost sensing for on-site fresh food analysis.

Keywords Molecularly imprinted polymers · Photopolymerization · Bisphenol A · Smartphone · Optical sensor · Food samples

Introduction

Bisphenol A (BPA) is an endocrine-disrupting chemical commonly detectable in various environmental samples [1]. It finds extensive use as a monomer within plasticizers, including materials such as polycarbonate, polyester resin, polysulfone, and epoxy resin. These substances are often employed in the production of consumer items like beverage containers, cans, water pipes, reusable bottles, and medical equipment. The mass production and widespread use of BPA have raised concerns about its release from plastic products and subsequent exposure to humans through various routes, such as skin contact, digestion, and inhalation, leading to potential

long-term health risks [2–5]. These risks encompass reproductive, immune, nervous, and metabolic problems and impacts on sperm production, fetal growth, anxiety, depression, and obesity. Certain processes involving hydrolysis, microwave heating, pasteurization, canning, packaging washing, and sterilization can increase the leaching of BPA into food products, further highlighting the importance of developing sensitive and selective detection methods to assess its toxicity [6–10].

In the realm of monitoring the endocrine-disrupting chemical BPA, an extensive array of reliable and sensitive analytical methods has come to the forefront. These methods, instrumental in scrutinizing BPA, encompass a diverse spectrum, with the most prevalent ones being spectrometry [11], high-performance liquid chromatography (HPLC) [12–14], gas chromatography (GC) [15, 16], mass spectrometry (MS) [17], capillary electrophoresis [18], electrochemistry [7, 19], and immunoassay [1, 20].

The broad spectrum of available methodologies reflects the multifaceted nature of BPA analysis. Each method contributes its unique strengths, with spectrometry providing a

✉ Aziz Amine
aziz.amine@fstm.ac.ma

¹ Laboratory of Process Engineering and Environment, Faculty of Sciences and Techniques, Hassan II University of Casablanca, 20650 Mohammedia, Morocco

versatile platform, HPLC offering precision, GC enabling separation of complex mixtures, MS delivering high sensitivity, capillary electrophoresis demonstrating efficiency in separation, electrochemistry showcasing electroanalytical capabilities, and immunoassay utilizing antibodies for specific BPA detection. Nevertheless, these analytical strategies are accompanied by certain constraints, including high expenses, intricate instrumentation, limited selectivity, time-intensive procedures, and a demand for skilled personnel. Moreover, BPA is commonly found in complex matrices, necessitating sample pretreatment. Conventional sample preparation methods like liquid–liquid extraction and solid-phase extraction pose challenges such as complex procedures, solvent usage, waste generation, and low selectivity [21]. This has driven the exploration of innovative extraction methods. Molecularly imprinted polymers (MIPs) have emerged as noteworthy candidates for precise recognition in biological and chemical sensors [22–24]. MIPs are artificial counterparts that emulate the antigen–antibody interactions observed in biological systems [25, 26]. These polymers possess distinct recognition sites that match the size, shape, and functional groups of their corresponding templates. In contrast to natural receptors, MIPs exhibit remarkable mechanical and chemical stability, substantial specific surface area, and cost-effectiveness in their production. As a result, MIPs have found widespread application across various domains, including chromatography [27], sample preparation, and biosensors [21, 28–31].

Various synthesis techniques for MIPs have been employed, including electropolymerization [23, 32], thermal heating [33], microwave irradiation [21], and sonochemistry, among others. Recently, photopolymerization has become a novel technique for synthesizing MIPs [34]. In this process, a light-sensitive system, known as a photoinitiator, triggers the polymerization of monomers upon light absorption, termed photo-polymerization. There are two main reasons for choosing photopolymerization. Firstly, the use of light allows for low temperatures, preserving non-covalent interactions between functional monomers and the template, leading to an increase in the efficiency of imprinting efficiency and a greater target affinity of MIPs. Additionally, low temperatures are preferred to protect sensitive analytes and avoid undesired side reactions. Secondly, photochemical processes enable precise control upon the polymerization chain aspects. By simply turning the light source on or off, radical generation can be instantly activated or halted, making photopolymerization more efficient compared to other synthesis strategies [35].

Recently, smartphone-assisted sensors have revolutionized colorimetric detection by combining advanced technology with practical convenience. Leveraging the camera's imaging capabilities, these sensors enable real-time, on-site analysis [36, 37]. The integration of smartphones with colorimetric assays eliminates the need for specialized equipment, making it accessible and cost-effective for

a wide spectrum of applications. This innovative approach has proven practical in fields such as environmental monitoring, medical diagnostics [38], and food safety testing, streamlining data collection and analysis processes [39].

To the best of our knowledge, a novel and innovative approach for the detection of bisphenol A in food samples using an integrated system that combines fast photopolymerized molecularly imprinted polymers with a smartphone-based colorimetric assay was first time proposed. The development of a UV-assisted synthesis method for BPA-imprinted polymers has led to significant improvements in efficiency and reduced synthesis time. The resulting MIPs exhibit remarkable selectivity for BPA over other interferents. The synergy between photopolymerized MIPs in solid-phase extraction (SPE) columns and smartphone-based optical sensing achieves selective, rapid, and affordable sample preparation tool, rendering it suitable for intricate food sample processing. This approach sets the stage for a straightforward and rapid sensing method for on-site analysis.

Materials and methods

Chemicals and reagents

In the context of MIP synthesis, the necessary reagents were procured as follows: BPA was used as the template molecule, methacrylic acid (MAA) with a purity of 99% was utilized as the functional monomer, 2,2 azobis (isobutyronitrile) (AIBN) served as the initiator, and ethylene glycol dimethacrylate (EGDMA) with a purity of 98% was used as the cross-linker, all obtained from Sigma-Aldrich (Germany). The porogen solvents, namely dimethylsulfoxide (DMSO) $\geq 99\%$ and acetone $\geq 99\%$, were sourced from Loba chimie (India).

For the selectivity study, gallic acid with a purity of 98%, along with sodium ions (Na^+), nitrite ions (NO_2^-), citric acid, vitamin C, nitrate ions (NO_3^-), zinc ions (Zn^{2+}), iron(II) oxide (Fe^{2+}), and sulfate Ion (SO_4^{2-}), were obtained from Loba chimie (India). For colorimetric BPA detection, sulfamethoxazole (SMX) $\geq 98\%$, sodium nitrite (NaNO_2) $\geq 99\%$, disodium hydrogen phosphate dodecahydrate ($\text{Na}_2\text{HPO}_4 \cdot 12 \text{H}_2\text{O}$) with a pH of 12.35 (utilized as the working buffer), and hydrochloric acid (HCl) with a concentration of 37% were sourced from Sigma-Aldrich (USA).

For the MIP extraction process, methanol $\geq 99.9\%$ and acetic acid $\geq 99\%$ were procured from Sigma-Aldrich (USA).

Apparatus and image processing

To synthesize the MIP, portable UV lamps with wavelengths of 395, 365, and 254 nm were purchased from Amazon. For

smartphone colorimetric sensing, images were captured using an A Xiaomi Mi 9T Android smartphone with a camera resolution of 48 megapixels (5000×3000). To detect BPA colorimetrically, 200 μL of the reaction mixture of the BPA standard or BPA-containing sample was dropped onto ELISA-plate microwells. Subsequently, signal readout involved using of a smartphone camera to perform RGB splitting. All images were hand captured from a predetermined and optimal distance from color spots, while ambient illumination conditions were maintained. To ensure reliability, each image was acquired in triplicate to facilitate the calculation of standard deviation (SD). For digital display and analysis, the images were subject to analysis employing the freely available ImageJ software. This facilitated the automatic calculation of color intensities across the red, green, and blue, RGB color spaces. In addition to this, absorbance measurements were executed using an ELx800 absorbance 96-microplate reader from BioTek Instruments (Winooski, USA). The measurements were conducted at a wavelength of 450 nm, thereby enabling the assessment of optical density related to the developed colorimetric yellow product. The ELx800 absorbance reader was also used for a comparison with the proposed smartphone method. Data were evaluated using Gen5 software, and the optical density of the yellow color of BPA was measured at 450 nm against the blank.

Fourier transform infrared (FTIR) spectra were acquired using a JASCO diamond ATR spectrometer (FT/IR-4600, Japan).

For the analysis of real-world samples, laboratory tap water was obtained, and commercial juice samples were procured from the market. The tap water was directly used as collected. However, the preparation of the juice samples necessitated the use of an Elmasonic ultrasonic bath (model S30(H), Germany), equipped with a thermostat. This specific equipment was chosen to ensure effective and accurate sonication of the juice samples, thereby achieving the best possible outcomes during the preparation procedure.

To facilitate the extraction and removal of the template molecule from the MIP, an empty polypropylene SPE tube equipped with polyethylene frits, featuring a 20- μm porosity and possessing a volume of 5 mL (sourced from Sigma-Aldrich, USA), was employed (see Electronic Supplementary Material Fig. S1). Additionally, for the purpose of BPA detection, another vacant polypropylene SPE tube was used. This tube was also equipped with polyethylene frits of 20 μm porosity and had a volume of 1 mL (obtained from Sigma-Aldrich, Germany). This specific SPE tube was dedicated to the SPE-MIP process (see Scheme 2).

Procedure for the colorimetric determination of BPA

A distinct diazotization solution is generated within a separate tube by meticulously combining equimolar portions of

sulfamethoxazole from stock solution of 4 mg mL⁻¹, hydrochloric acid (at 2 M), and sodium nitrite solution (at a stock concentration of 23 mg mL⁻¹). Then, the mixture is gently swirled for a duration of 5 min at room temperature. Subsequent to this process, 60 μL of the pre-prepared diazotization solution is introduced to a solution containing 1 mL of BPA. This is followed by the gradual addition of 100 μL of phosphate buffer (at a concentration of 0.5 M, pH = 12.3) into the mixture, adhering to a sequential order as prescribed [11]. The degree of the resultant yellow color development is directly proportional to BPA concentration. To measure the absorbance of the final yellow solution, a comparison is made against a reagent blank. This measurement can be undertaken by employing either a microplate reader at a wavelength of 450 nm or alternatively, by utilizing a smartphone.

Photopolymerization of monomer to produce MIPs for BPA

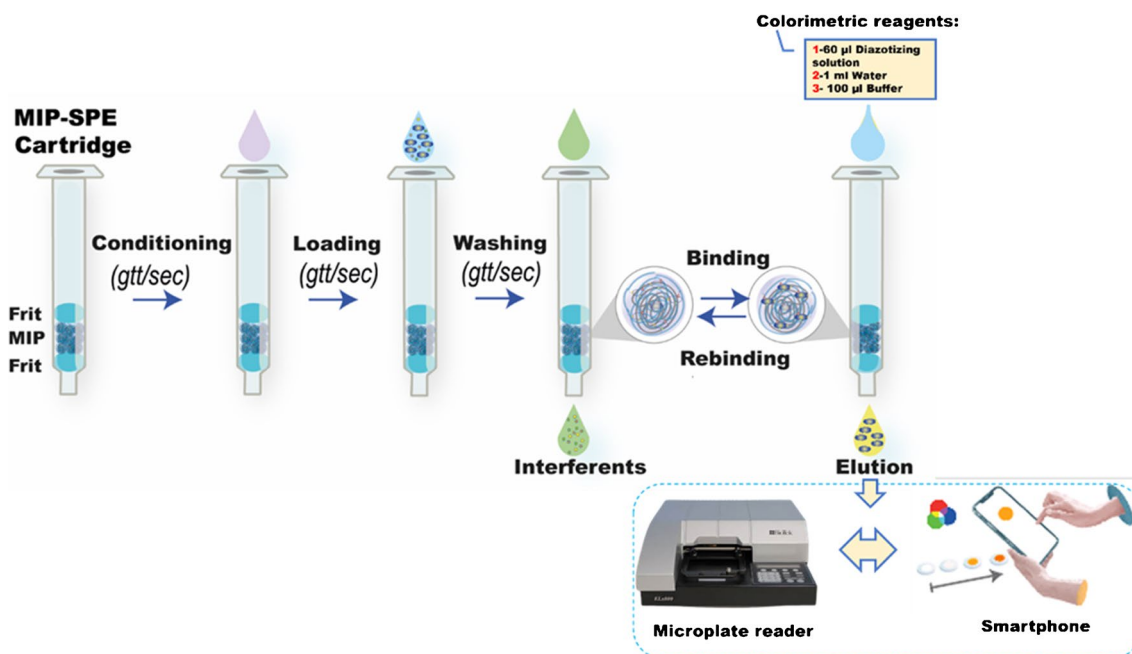
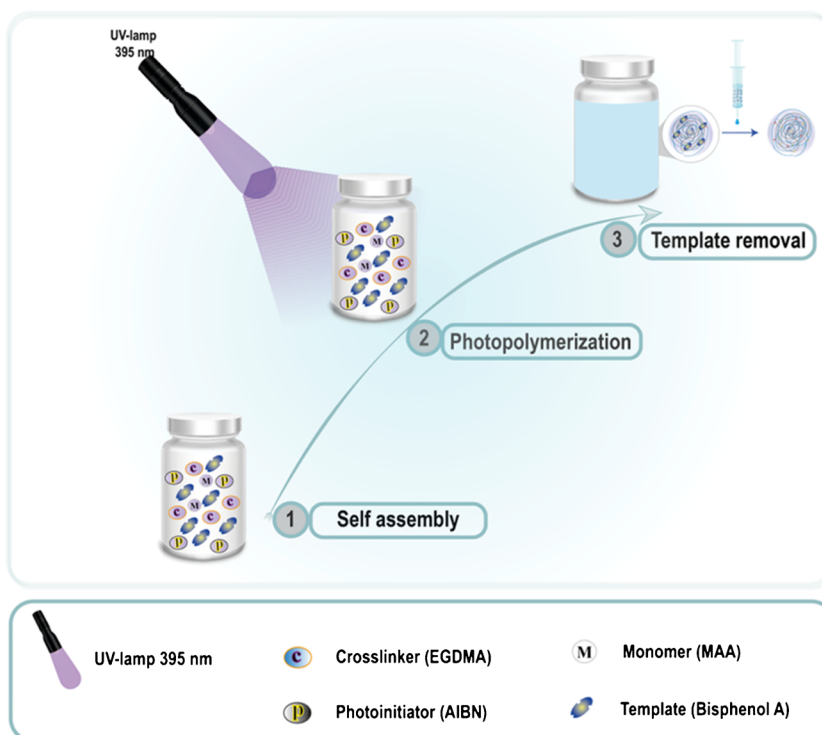
The development of MIPs based on UV synthesis for BPA was on the basis of a multistage procedure (see Scheme 1).

In the synthesis of BPA-MIP, BPA served as the template, MAA acted as the monomer, EGDMA was used as the cross-linker, AIBN functioned as the initiator, and Acetone acted as the porogen solvent. In brief, the synthesis procedure involved dissolving 2.3 mg of BPA and 35 μL of the functional monomer MAA in 0.2 mL of acetone in a 5-mL glass vial. The solution was then left to incubate in darkness at 4 °C for 2 h to facilitate the formation of hydrogen bonds between MAA and BPA.

Next, 1.6 mL of DMSO, 64 μL of the cross-linker EGDMA, and 4 mg of the initiator AIBN were added to the previous solution, along with 0.3 mL of H₂O. The polymerization reaction was initiated using a UV lamp (395 nm) within a dark box, lasting for 20 min (see Electronic Supplementary Material Fig. S2). Following the polymerization, the BPA template was removed from the synthesized MIP through multiple extractions using a mixture of methanol and acetic acid (9:1) until BPA was no longer detectable via UV spectrophotometry at 280 nm. Subsequently, the collected material was washed with water to eliminate any remaining traces of the extraction solvent. Next, the polymer was dried in the oven at 45 °C and then was suspended in water to reach a final concentration of 1 mg per 200 μL . Subsequently, 200 μL of this suspension of MIP or NIP was added to each solid-phase extraction (SPE) cartridge with a maximum capacity of 1 mL. Next, a SPE syringe with a specific adapter was used to drive the liquid out of the SPE creating a MIP/NIP layer ready for sample loading (see Electronic Supplementary Material Fig. S1).

As for the non-imprinted polymer (NIP), it was synthesized using the same procedure but without the addition of BPA. Finally, both the resulting MIP and NIP were dried in an oven at 45 °C.

Scheme 1 Generic scheme for the UV-mediated fabrication of BPA-photopolymerized MIP



Scheme 2 Generic scheme of the MIP-SPE of BPA procedure

MIP-solid-phase extraction (MIP-SPE)

A method for SPE-MIP was successfully developed, employing photopolymerized MIPs as the specific sorbent material within the SPE columns. In this approach, a 1-mL SPE cartridge was filled with 200 µL each of

the suspended MIP and NIP (1 mg in 200 µL), positioned between two polyethylene frits. The procedure encompasses four clearly defined steps, as delineated in Scheme 2: (a) initial conditioning of the cartridge using 1 mL of water, (b) sequential loading of the BPA standard (or sample extract) in water, (c) subsequent washing

of the cartridge with 1 mL of water, and (d) concluding with elution, which involves 1 mL of the colorimetric reagents. In this elution step, a mixture of the colorimetric reagents containing 60 μ L of diazotizing solution, 1 mL of water, and 100 μ L of buffer was used. The resulting yellow elution solution corresponds proportionally to the BPA retained in the cavities.

Simultaneously, a standard loading solution with varying concentrations of BPA is prepared, using the same colorimetric strategy. This step is undertaken to evaluate the performance of MIP and NIP relative to the standard. Additionally, it also enables the calculation of the extraction recovery for the entire sensing strategy. The calculation of extraction recoveries was carried out using the subsequent equation as a fundamental methodology [40, 41]:

$$R\% = \frac{C_f}{C_i} \times 100 \quad (1)$$

In this particular context, the symbol “ C_i ” corresponds to the initial concentration of BPA, whereas “ C_f ” represents the concentration of BPA after the completion of the extraction process.

Scheme 1 illustrates the solid-phase extraction (MIP-SPE) procedure.

Binding experiments

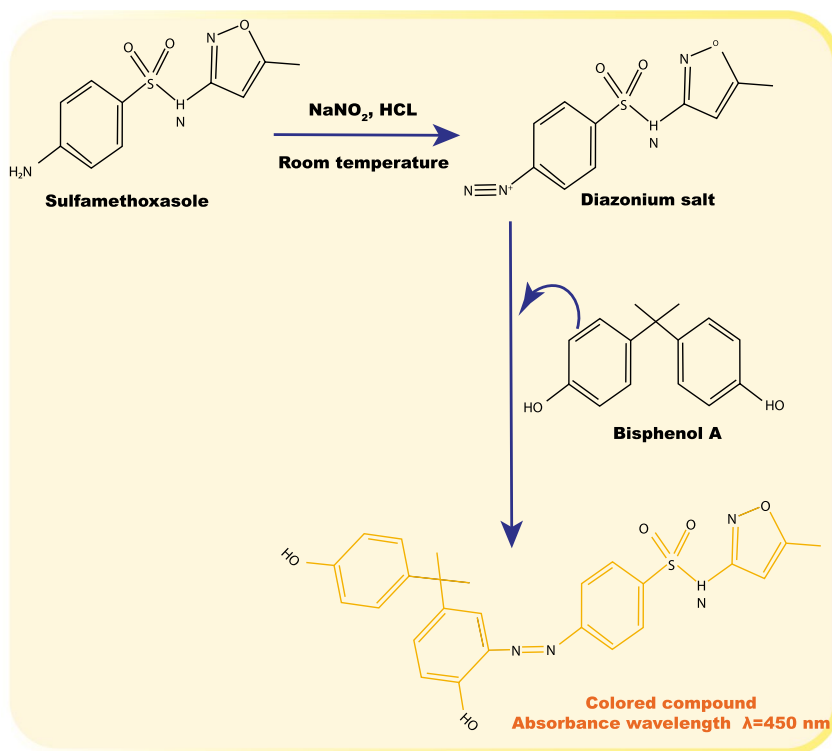
The series of binding experiments was diligently executed in strict adherence to the procedure methodically detailed in “MIP-solid-phase extraction (MIP-SPE)” section. These

experiments were deliberately carried out utilizing both MIP and NIP-based cartridges to ensure a comprehensive and comparative investigation. To this end, solutions characterized by progressively escalating concentrations of BPA were accurately prepared. The concentration range spanned from 0.25 to 10 ppm and was effectively dissolved in a water-based medium. The controlled loading of these solutions into the experimental setup was achieved with a consistent volume of 1 mL.

The quantification of the concentration of BPA present within the supernatant was conducted employing a precisely executed colorimetric technique [14]. This method necessitated the strategic combination of SMX and BPA within the presence of NaNO_2 and HCl. This reaction orchestrated the formation of a distinctive diazonium salt, an intermediate compound. Subsequently, this diazonium salt underwent a controlled alkalization process under the influence of the working buffer. This particular manipulation resulted in the transformation of the intermediate compound into a distinctive, yellow-colored compound. The quantification of the absorbance of this yellow compound was performed at a precisely determined wavelength of 450 nm, utilizing the sophisticated measurement capabilities of a dedicated microplate reader. The intricate mechanism underlying the operation of this colorimetric methodology is effectively elucidated through the graphical representation provided in Fig. 1.

The determination of the equilibrium adsorption capacity, an indispensable parameter in the study, for both MIPs and NIPs (expressed as Q in units of mg/g) was accomplished utilizing the following equation [42]:

Fig. 1 Mechanism of the coupling reaction between BPA and the diazonium salt of sulfamethoxazole [11]



$$Q_e = \frac{C_i - C_e}{m} \times V \quad (2)$$

This equation effectively serves to determine the equilibrium adsorption capacity (Q) and involves the utilization of the initial concentration (C_i) and the final concentration (C_f) of the solute in mg/L. The parameters V and m , respectively, represent the volume of the loading solution in liters (mL) and the mass of the imprinted polymer in grams (mg).

The characterization of the specific recognition capabilities inherent within the synthesized MIPs was effectively accomplished through the utilization of a critical parameter known as the imprinting factor (IF). The formula to calculate the imprinting factor (IF) is as follows [43]:

$$IF = \frac{QMIP}{QNIP} \quad (3)$$

This particular factor (IF) is essentially established through the utilization of the adsorption capacities of both the MIP ($Q(MIP)$, measured in mg/g) and NIP ($Q(NIP)$, also measured in mg/g).

The comprehensive analysis of the adsorption isotherm was obtained through a systematic variation of the initial loading concentration of BPA, precisely ranging from 0.25 to 20 mg/L. This strategic modulation of the adsorbate's initial concentration provided a comprehensive depiction of the relationship between the adsorbate's quantity and the resulting equilibrium concentration within the experimental system.

Determination of BPA in food samples

Juice samples were obtained from a local market source. A volume of 2.5 mL from each sample was diluted by adding 7.5 mL of water and subsequently subjected to a 5-min sonication process within an ultrasound bath. To assist in the dissolution of sugars, the solution was subsequently subjected to a warming process at a temperature of 50°C for a duration of 30 min. Following this step, the resultant solution underwent centrifugation, and the supernatant was methodically filtered using a micropore filter membrane with a pore size of 0.45 μm . Once this filtration process was complete, the filtrate was carefully transferred to a designated volumetric flask. The volume of this filtrate was precisely adjusted with water to attain a final volume of 25 mL. It was imperative to ensure the accuracy and uniformity of the sample volume for further analysis.

For tap water samples, a distinct procedure was followed. The tap water samples were directly utilized as they were collected, without the need for any additional treatment steps.

The obtained pH values for both the investigated juice and tap water samples were 4.02 and 7.52, respectively.

Results and discussion

Photosynthesis of MIPs for BPA

The optimization of photopolymerization parameters for MIPs using different light sources led to significant improvements. When a 254 nm UV lamp was used under the given duration and synthesis conditions, no polymer was obtained. However, the implementation of efficient UV lamps (395 nm and 365 nm) successfully reduced the overall synthesis time. Within the initial 5 min, the polymerization reached an intermediate stage, showing promising progress. By 20 min, total polymerization was achieved, indicating the formation of well-developed MIPs (see Electronic Supplementary Material Fig. S2).

This remarkable reduction in time, while maintaining the desired level of polymerization efficiency, highlights the effectiveness of UV-assisted synthesis for MIPs. It opens the path for faster production and potential applications in various fields. Interestingly, utilizing sunlight as a light source also showed promising results. Within the first 20 min, the polymerization reached an intermediate stage, and by 30 min, total polymerization was achieved, leading to the formation of well-developed MIPs. The specific parameters used, and the resulting MIPs yield are detailed in Table S1 (see Electronic Supplementary Material Table S1).

The explanation for this phenomenon revolves around the photoinitiator's characteristics. It exhibits (i) a significant absorption coefficient at the chosen irradiation wavelength, enabling efficient generation of excited states (singlets); (ii) an efficient internal conversion from singlet states to dissociative triplet states, resulting in radical formation through bond cleavage; and (iii) the generation of highly reactive photons, leading to excited states capable of producing reactive radicals that trigger monomer polymerization. The choice of UV wavelength depends on the specific photoinitiator being used, with common wavelengths for photopolymerization being 365 nm and 395 nm.

In UV MIP photopolymerization using AIBN (Azobisisobutyronitrile) as the initiator (note that AIBN can also act as a photoinitiator in the UV range of 320–400 nm in addition to its thermal initiation), UV light is absorbed by AIBN, leading to the formation of free radicals that initiate the polymerization process [35, 44]. Upon excitation, the photoinitiators undergo a process of unimolecular homolytic bond cleavage to generate radicals. During polymerization, MAA interacts with BPA, creating specific recognition sites within the polymer matrix. EGDMA, as a cross-linking agent, contributes to the formation of a stable three-dimensional network. After completion, the template is removed, resulting in MIPs with complementary binding sites for BPA. This approach provides precise control, fast

reaction rates, and high affinity and specificity towards the target molecule.

To identify the optimal UV lamp for efficient MIP production, both 395 nm and 365 nm UV lamps were employed to create MIP and NIP for bisphenol A. The comparison focused on evaluating cavity creation efficiency. Through binding performance and imprinting factor calculations, it was found that the MIP produced with the 395 nm UV lamp outperformed the one generated with the 365 nm lamp. The MIP created using the 395 nm UV lamp exhibited an imprinting factor of 3.0 ± 0.05 (with a relative standard deviation of $\leq 6\%$ and $n = 3$), while the MIP produced with the 365 nm UV lamp showed an imprinting factor of 1.58 ± 0.03 . In this study, a UV lamp emitting light at 395 nm was selected as the most suitable option for generating BPA MIPs.

MIP extraction optimization

The crucial step in MIP synthesis involves the removal of the template used to shape the cavities. Factors like unsuitable binding site affinity, low template solubility, and the cross-linked network make the removal challenging. Incomplete template removal reduces cavity availability, decreasing imprinting efficiency. New techniques aim to enhance removal efficiency, reduce time, and minimize environmental impact. Despite its importance, template removal receives limited scientific attention compared to other steps, making it the least cost-effective aspect of MIP synthesis. The difference in template and polymeric matrix properties drives extraction strategies. Essential parameters for assessing extraction methods include environmental impact, cost, solvent consumption, complexity, operation time, and commercial potential. The choice of extraction technique relies on template and MIP network stability and nature.

In this study, we introduced a fast and cost-effective method for template removal using solid-phase extraction (SPE) (see Electronic Supplementary Material Fig. S3). Indeed, the obtained polymer (250 mg) was introduced into 5 ml SPE columns, and a series consecutive extraction cycles were conducted. In each cycle, a 2 mL mixture of methanol and acetic acid (in a ratio of 9:1) was employed as the loading solvent. These cycles were carried out repeatedly until BPA could no longer be detected using UV spectrophotometry. The efficiency of the process was evident as 10 cycles with the extraction solvent effectively removed BPA from the MIP. The material was then washed with water three times to eliminate any residual extraction solvent. Following that, the polymer was dried in the oven at 45 °C and then was suspended in water to achieve a final concentration of 1 mg per 200 μL . Subsequently, 200 μL of this suspension of MIP or NIP was added to each SPE cartridge with a maximum capacity of 1 mL. This step aimed to facilitate

and minimize errors that could occur by directly adding 1 mg of the polymer into each individual SPE cartridge. The proposed SPE-based strategy for BPA removal showed reproducibility in MIP performance and allowed rapid and economical template removal compared to conventional Soxhlet or solvent incubation elution methods, which can take several hours to days.

MIP performance

The MIP and NIP equilibrium adsorption capacities for BPA were thoroughly examined, varying the initial concentration of BPA as shown in Fig. 2.

The MIP showed a higher affinity for BPA than the NIP, as the BPA uptake by the MIP increased significantly with the BPA concentration. This implies that the MIP had specific binding sites that matched the BPA molecules. The MIP-SPE method also demonstrated excellent repeatability for all BPA levels tested ($\text{RSD} \leq 6\%$, $n = 3$), indicating its reliability. The MIP had an IF of 3.02 ± 0.05 , which reflects its superior performance in comparison to NIP.

FT-IR characterization

The characterization technique utilized in this study involved the application of FTIR analysis to examine the studied materials. In the FT-IR spectra of both the NIP and the MIP, as depicted in Fig. 3, distinct features were observed. Notably, the peaks at 1726 cm^{-1} and 1157 cm^{-1} were identified. These characteristic peaks can be attributed to the presence of key functional groups within the polymethacrylic structure. Specifically, the peak at 1726 cm^{-1} corresponds to the

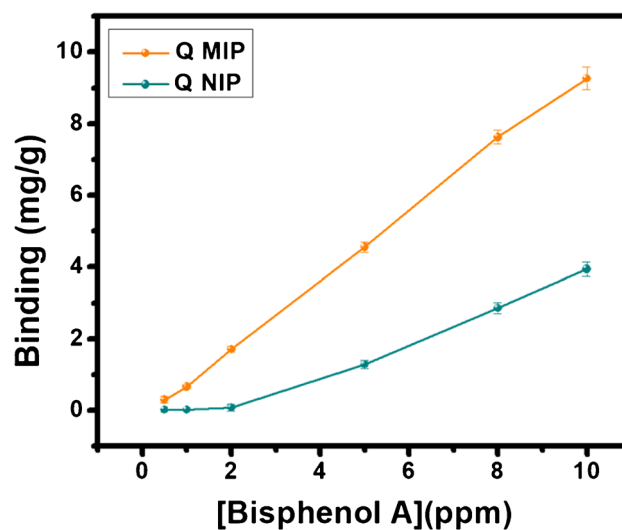


Fig. 2 Binding adsorption isotherms achieved with MIP and NIP for BPA

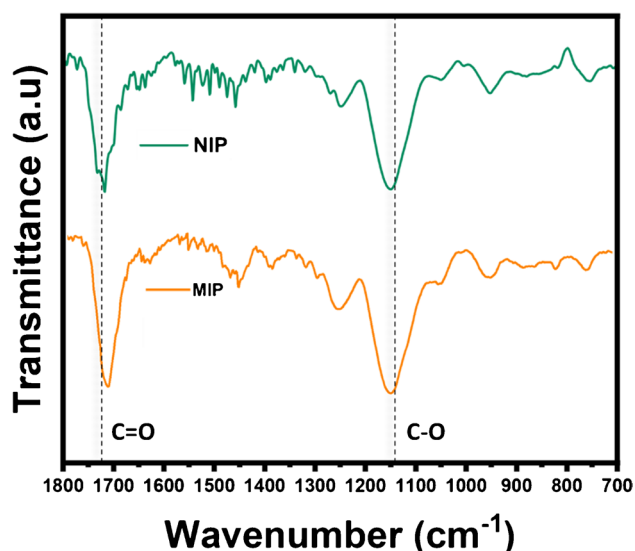


Fig. 3 FT-IR spectroscopic analysis of extracted molecularly imprinted polymer for bisphenol A (MIP-BPA) and non-imprinted polymer (NIP)

C=O functional group, signifying the presence of carbonyl groups within the polymer structure. Likewise, the peak at 1157 cm^{-1} corresponds to the C-O single bond functional

group, demonstrating the existence of oxygen-carbon linkages. These findings collectively indicate the successful preparation of the polymer, and the distinctive FT-IR spectra provide valuable insights into the structural composition and chemical characteristics of both the NIP and MIP materials.

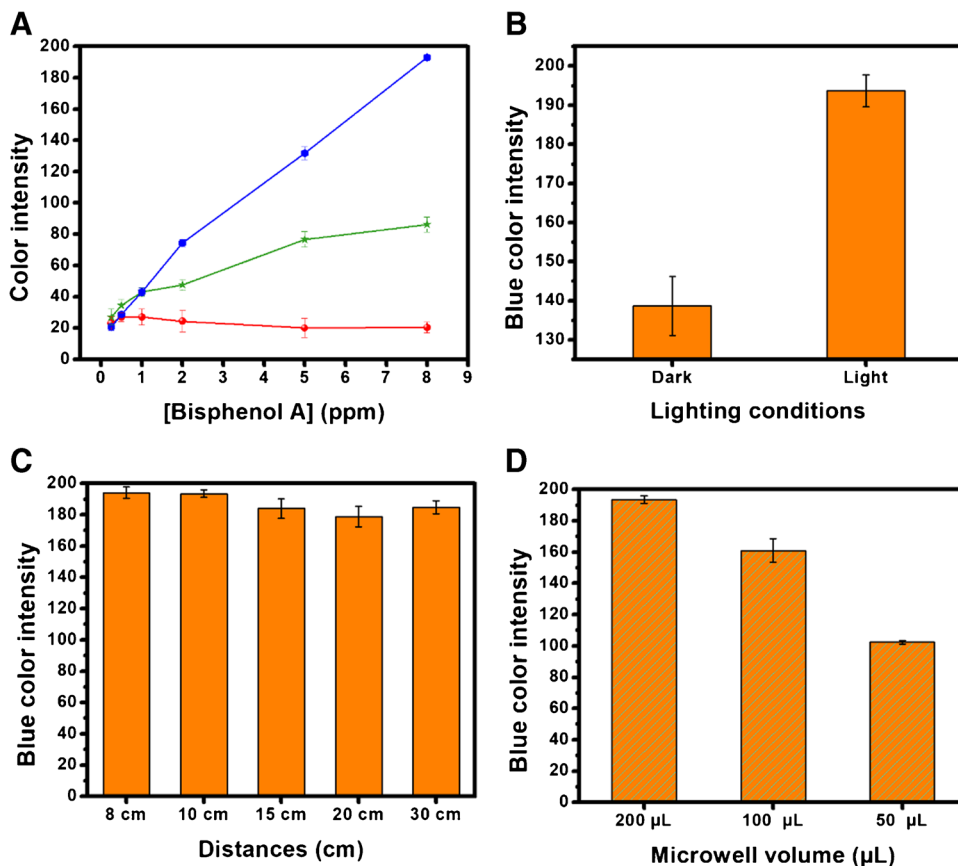
Analytical determination of BPA

Detection based on photometry

A comprehensive analysis was conducted encompassing a variety of concentrations of BPA, strategically varying from 0.25 to 10 mg/L. The quantification process was carried out through the utilization of a microplate reader, with measurements taken at a precise wavelength of 450 nm. The resultant outcomes were aptly depicted in Figure S3, where a detailed dose–response curve was successfully constructed, leveraging the equation established for the linear range. This representation offers a comprehensive visual insight into the relationship between the concentrations of BPA and the observed responses.

The critical parameters of limit of quantification (LOQ) and limit of detection (LOD) were skillfully determined as

Fig. 4 **A** Correlation between red, green, and blue color values corresponding to BPA concentrations ranging from 0.25 to 8 ppm. **B** Comparison of blue color intensities under dark conditions (flashlights on) and well-illuminated conditions. **C** Variation of blue color intensities relative to different focal distances between the microwell and smartphone camera. **D** Influence of varying BPA solution volume within the microwell on blue color intensities. Data are presented as mean \pm standard deviation (SD), with $n = 3$ replicates



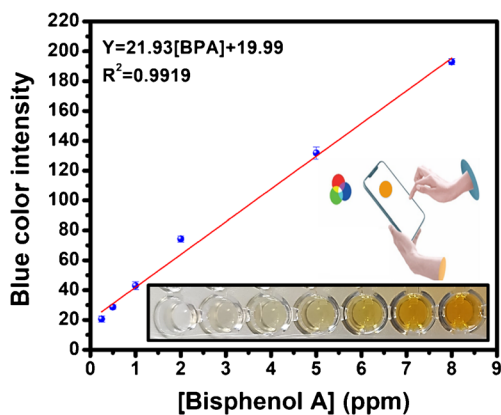


Fig. 5 Calibration plot illustrating the correlation utilized to quantify BPA through the smartphone-based optical detection method

part of the analysis. The LOD, was determined to be 0.1 mg/L. Likewise, the LOQ was found to be 0.3 mg/L.

The computation of these limits followed specific formulas. The LOD was calculated using the formula $LOD = 3\sigma/b$, where σ symbolizes the standard deviation of the intercept, and b represents the slope of the calibration curve. Similarly, the LOQ was determined using the formula $LOQ = 10 * \sigma/b$. These formulas, involving statistical measures of variability and the slope of the calibration curve, are fundamental in

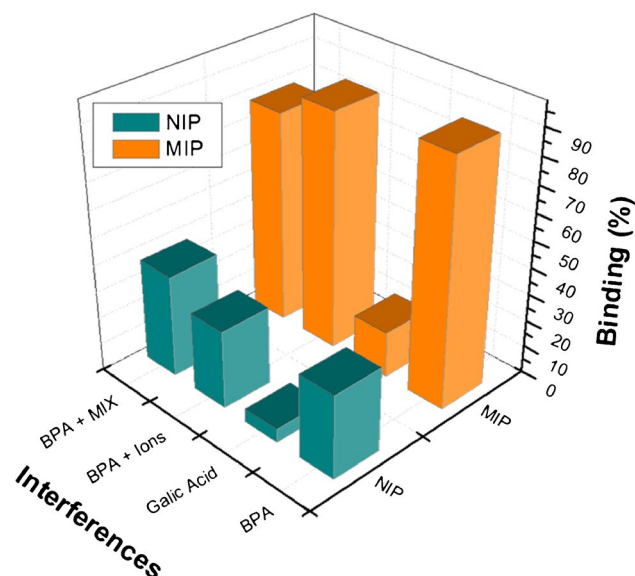


Fig. 6 Selective adsorption profiles of the photopolymerized molecularly imprinted polymers (MIPs) and non-imprinted polymers (NIPs) demonstrated for bisphenol A (BPA) (5 ppm), Gallic acid (5 ppm), a composite ionic mixture comprising BPA (5 ppm); Na⁺ (50 ppm); NO₂⁻ (25 ppm); NO₃⁻ (50 ppm); Zn²⁺ (50 ppm); Fe²⁺ (50 ppm); SO₄²⁻ (50 ppm), and a composite mixture comprising BPA (5 ppm); gallic acid (50 ppm); Na⁺ (50 ppm); NO₂⁻ (25 ppm); citric acid (50 ppm); Vitamin C (50 ppm); NO₃⁻ (50 ppm); Zn²⁺ (50 ppm); Fe²⁺ (50 ppm); SO₄²⁻ (50 ppm)

establishing reliable thresholds for detection and quantification within the analytical framework.

Smartphone detection

To rigorously define the parameters for smartphone-based detection, an intricate series of experiments were systematically conducted, with the primary objective of establishing optimal conditions. Initially, a range of color reactions was carefully prepared, involving BPA solutions, and subsequently placed within microwells of an ELISA plate. To capture the necessary imagery, a smartphone was employed, with considerable attention given to varying conditions to ensure comprehensive assessment. These encompassed diverse distances from the smartphone's lens, namely 8, 10, 15, 20, and 30 cm, as well as different volumes allocated to each microwell, with options of 50, 100, and 200 μ L. Moreover, two distinct lighting scenarios were explored: one with an active smartphone flashlight and one without.

In this intricate process, color intensities were judiciously computed across various color spaces, and the powerful Image J software was harnessed perform direct color channel analysis using the smartphone imagery. The resultant color intensities were methodically plotted in relation to the corresponding BPA concentrations, a visual representation found in Fig. 4A. These color intensities were specifically examined across red, green, and blue color spaces, with each space being individually assessed concerning its response to varying BPA concentrations. Notably, the blue color space demonstrated a compelling decline in intensity as BPA concentration increased, indicative of heightened sensitivity in this channel. Consequently, based on this insightful observation, the blue color space was designated as the most optimized quantitative analytical parameter among all the color spaces tested. In the quest

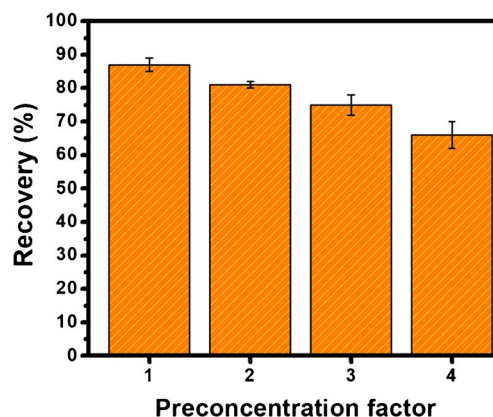


Fig. 7 Impact of loading volume on extraction recovery in preconcentration factor study (1 ppm BPA; 1, 2, 3, 4 mL loading volumes with 1 mL elution volume)

Table 1 Concentrations (ppm) of BPA in water, 1% HCL, 1% NaOH and juice in different PC cup heated under microwave for 5 and 15 min

Plastic type	Volume (mL)	Migration at T0	Migration under microwave for 5 min	Migration under microwave for 15 min
PC	100 mL water	Not detected	Not detected*	Not detected*
PC	100 mL (1% HCL)	Not detected	Not detected*	Not detected*
PC	100 mL (1% NaOH)	Not detected	0.7 ppm	0.9 ppm
PC	100 mL (1/10 juice sample)	Not detected	0.6 ppm	0.7 ppm

Polycarbonate (PC)

*not detected (\leq LOD)

to identify the most suitable image acquisition conditions, two distinct lighting scenarios were rigorously compared: images taken under natural daylight and those captured within a controlled dark box environment, with external light sources activated (flashlights on). The outcomes from this comparison unequivocally favored the images acquired under natural daylight conditions due to their superior sensitivity, as illustrated in Fig. 4B. Further refinement of the imaging conditions encompassed the careful manipulation of the distance between the smartphone's camera lens and the microwell. This exploration aimed to pinpoint the distance that yielded the most reliable results. By measuring the intensity of the blue color channel across varying distances (ranging from 8 to 30 cm), it was ascertained that a distance of 10 cm provided optimal results, consistently displaying higher color intensity compared to the other tested distances, namely 15, 20, and 30 cm, as illustrated in Fig. 4C. Moreover, the impact of varying the BPA volume per microwell was also methodically examined, encompassing a range from 50 to 200 μ L. The outcome of this assessment highlighted that a volume of 200 μ L exhibited enhanced sensitivity, as illustrated in Fig. 4D.

In summation, after thorough analysis and thoughtful consideration of these various factors, the most favorable imaging conditions were definitively identified as follows: a microwell volume of 200 μ L, a focal distance of 10 cm, image acquisition conducted in natural daylight, and the interpretation of data based on the blue color channel. This comprehensive assessment ensures optimal conditions for reliable and accurate smartphone-based BPA detection.

Figure 5 illustrates the BPA calibration curve obtained using the smartphone with the blue color channel.

The obtained results revealed a linear range from 0.25 to 8 mg/L, with a determination coefficient (R^2) of 0.9919. The LOD and LOQ were found to be 0.144 and 0.482 mg/L, respectively. A comparison between the microplate reader at 450 nm and smartphone detection showed no significant difference in performance. However, using the smartphone for detection offers the advantages of rapid analysis, cost-effectiveness, and the ability to perform in-field testing without compromising sensitivity.

Selectivity study

To comprehensively evaluate the selectivity of the MIPs, an intricate series of tests were systematically conducted involving a variety of compounds. Of particular interest were the assessments of mixtures containing BPA in the presence of Gallic acid (5 ppm), as well as a composite mixture composed of BPA (5 ppm), Gallic acid (50 ppm), Na^+ (50 ppm), NO_2^- (25 ppm), citric acid (50 ppm), Vitamin C (50 ppm), NO_3^- (50 ppm), Zn^{2+} (50 ppm), Fe^{2+} (50 ppm), and SO_4^{2-} (50 ppm). The multifaceted outcomes derived from these extensive examinations have been punctiliously documented and presented in Fig. 6, providing a detailed insight into the MIPs' distinctive selectivity characteristics across this diverse array of compounds.

The thorough analysis assessing the selectivity of MIPs and NIPs (as depicted in Fig. 6) unequivocally supports the successful creation of specialized recognition sites within the synthesized MIP structure, designed exclusively for BPA interaction. This validation is reinforced by the significant increase in MIP's uptake capacity for BPA compared to the relatively lower affinities with gallic acid. The adsorption capacities of MIPs and NIPs exhibit similar responses to gallic acid, but a notable difference emerges for BPA. This difference highlights the role of meticulously engineered template-shaped cavities unique to the

Table 2 Data obtained by analyzing fortified tap water and samples juice extracted using the MIP-SPE

BPA added (mg/L)	BPA found (mg/L)	Recovery (%)
Tap water		
0.5	0.48 \pm 0.05	96
1	0.95 \pm 0.03	95
5	4.8 \pm 0.6	96
Juice		
0.5	0.45 \pm 0.02	90
2	0.17 \pm 0.04	84
5	3.4 \pm 0.6	68

Table 3 Comparative table of chemically synthesized MIPs for bisphenol A detection in real food samples

MIP polymerization technique	Synthesis time	Extraction time	IF	Detection method	LOD (ppb)	Real sample	Recovery	Ref
Commercial MIP cartridges (AffinimipVR Bisphenol)	-	-	-	UPLC with fluorescence detection	0.15 ppb	Canned energy drinks	78–94	[45]
Free radical chemical synthesis	60 °C /24 h	-	-	capillary electrophoresis	-	Milk	80–85%	[18]
Free radical chemical synthesis	-	-	3.60	HPLC–DAD*	3 ppb	Alcoholic and non-alcoholic beverages	89–107%	[12]
Surface-imprinted core–shell magnetic beads	70 °C for 24 h	-	-	HPLC	3.7 ppb	Milk	98.07% -99.21%,	[14]
Surface imprinting	18 h	-	-	HPLC	3 ppb	Tea Mineral water Fruits	98% to 105%	[46]
Surface imprinting	24 h	Soxhlet extraction	1.18	HPLC	0.02 ppb	Milk	89.9 to 102.5%	[47]
Copolymerization	6 h	Soxhlet extraction for 5 h	-	HPLC–DAD*	0.02 ppb	Juice, honey, milk and tomato paste	94.9–99.4%	[48]
Free radical photopolymerization	20 min	SPE extraction for 30 min	3	Smartphone-based Optical Sensing	30 ppb	Juice and tap water	68% to 96%,	This work

*High-performance liquid chromatography with diode-array detection (HPLC–DAD)

MIP structure, affirming its heightened affinity for BPA and establishing it as the primary recognition site for this target molecule. The BPA solution containing interfering ions showed only a slight change in adsorption capacity (less than 5%) compared to the pure BPA solution, indicating the MIP's excellent selectivity. This can be attributed to the abundance of imprinted cavities in the BPA-MIP, which exhibit strong chemical and structural affinity for BPA. These cavities enable BPA to be strongly bound within the polymer system, demonstrating a high affinity.

Preconcentration

SPE is frequently employed as a preconcentration or separation technique, especially when dealing with complex matrices or low analyte concentrations that require analysis. Preconcentration helps enhance the detection and quantification of the target analyte, making it a vital and integral step in numerous analytical procedures [15]. The examination of real samples using preconcentration underscores the significance of sample volume and elution volume in achieving notable preconcentration factors. As such, this study aimed to investigate the impact of loading volume on the recovery of the extracted analyte. The outcomes of this investigation are graphically presented

in Fig. 7, illustrating the relationship between sample loading volume and the subsequent recovery of the analyte. The preconcentration factor was determined by calculating the ratio of the sample charged volume (1, 2, 3, 4 mL) to the elution volume (1 mL). Loading 1 mL of 1 ppm BPA and eluting in 1 mL resulted in a recovery of 88%. Similarly, loading 2 mL of 1 ppm BPA and eluting in 1 mL gave a recovery of 81%, loading 3 mL resulted in 78% recovery, and loading 4 mL showed a recovery of 70%. The MIP demonstrated no significant losses up to a concentration factor of 4 times.

With a preconcentration factor of “4,” a theoretical LOD of 0.030 mg/L could be achieved.

Figure 7 illustrates the preconcentration factor study, investigating the impact of different loading volumes (1 ppm BPA; 1, 2, 3, 4 mL) on extraction recovery, with a constant elution volume of 1 mL.

Migration of BPA from plastic packaging

Polycarbonate (PC), polyethylene terephthalate (PET), and polypropylene (PP) plastics underwent an experiment to test for the migration of BPA. Each bottle was filled with water to its capacity and placed in an oven at 45°C. After incubating for 7 days, water samples (1 mL) were taken from each bottle and analyzed.

The results indicated no BPA leaching in any of the tested bottles (see Electronic Supplementary Material Table S2). This suggests that PET and PP plastics do not contain BPA. Interestingly, even in PC plastic, no BPA release was detected (or below the detection limit (0.1 ppm)). This lack of BPA release might be attributed to the migration conditions not being extreme enough to allow BPA release. To confirm this hypothesis, another experiment was conducted using 4 PC cups with different samples, and the release was studied under microwave conditions for 5 and 15 min. The results showed BPA release from PC when using Juice and a 1% NaOH solution (Table 1).

Real samples

In order to evaluate the practicality of the established methodology in real-world scenarios, the analysis of BPA was extended to encompass juice and tap water samples. Through the introduction of three distinct BPA concentrations into these samples, each underwent the conscientiously fine-tuned MIP-SPE protocol before undergoing analysis via the photometric-based approach. The outcomes of this analytical endeavor have been succinctly collated and are thoughtfully presented in Table 2, offering a comprehensive insight into the effectiveness and versatility of the developed methodology when applied to real sample matrices.

The obtained data validates the suitability of the MIP-SPE procedure for real sample analysis. The method exhibits reliable BPA quantification with recoveries ranging from 68 to 96%, and the low RSD ($\leq 6\%$) demonstrates the excellent reproducibility of the proposed sensing approach.

To the best of our knowledge, this is the first report that deals with the combination of sample clean up using a plastic antibody (MIP) synthesized by photopolymerization and smartphone determination of BPA in real food samples. Compared to the existing methods for the determination of BPA in real samples (Table 3), the main advantage of the proposed method lies in the fact that (i) the smartphone-based colorimetric detection, allowed simple, rapid, and low cost BPA analysis. Eventually, the applicability of the proposed strategy was proved for BPA quantification in different foods with a good recovery. (ii) In contrast to current strategies for the chemical synthesis of BPA MIPs, the proposed MIP formation process is rapid (20 min) and well-suited for efficient mass production of MIPs. Furthermore, in addition to the swift synthesis, a rapid template extraction from the MIP (30 min) is suggested, representing a shorter duration compared to the existing literature methods. (iii) Existing methodologies on the use of MIPs for BPA analysis in food (Table 3), especially those employing HPLC and robust techniques, achieve a low LOD. However, they come with several constraints, such as high costs, complex instrumentation, time-intensive procedures, and the need for skilled personnel. In our approach, the combination of smartphone analysis with preconcentration procedures via MIP enables the measurement

of BPA at lower limits, effectively addressing some of these challenges. (iv) The extraction of MIP using SPE columns with multiple cycles significantly reduced the extraction time to only 30 min (v) the main advantage of our strategy remains in the combination of sample cleanup by using MIP and the fast and affordable readout method for on-site food safety monitoring.

Conclusions

To conclude, the innovative synergy achieved by combining photopolymerized MIPs within SPE columns and smartphone-based optical sensing presents a novel and effective approach that encompasses selectivity, rapidity, and cost-efficiency in sample preparation. This revolutionary strategy not only paves the way for a straightforward and swift sensing method ideally suited for on-site analysis but also introduces a new extraction method that significantly shortens template removal time to a mere 30 min, thanks to the utilization of SPE columns with multiple cycles.

The MIP's proficiency as a potent adsorbent for solid-phase extraction is further enhanced by its integration with a colorimetric smartphone detection system, effectively demonstrating its good sensitivity for BPA detection. Additionally, a mere 5-min microwave treatment proves instrumental in releasing BPA from polycarbonate packaging in both juice and basic solutions. The integration of MIP-based selective sample preparation with colorimetric detection yields exceptional reproducibility ($RSD \leq 6\%$, $n = 3$) and specificity in quantifying BPA across various contexts, spanning model solutions and real food samples like juice and tap water.

In a remarkable testament to its utility, this cost-effective and swift MIP production methodology emerges as a powerful tool for conducting economical sensing analyses on real samples, thus addressing concerns surrounding BPA in the realm of food safety.

Supplementary Information The online version contains supplementary material available at <https://doi.org/10.1007/s00216-024-05212-0>.

Acknowledgements The authors acknowledge the EU-PRIMA-FED-KITO project—Fresh food sustainable packaging in the circular economy.

Author contribution Conceptualization; formal analysis; methodology; investigation; writing, original draft; and figure drawings: D.E. Conceptualization; supervision; visualization; reviewing and editing; validation; and project administration: A.A. All authors have read and agreed to the published version of the manuscript.

Funding This work was supported by EU-PRIMA-FEDKITO project—Fresh food sustainable packaging in the circular economy.

Declarations

Ethics approval Not applicable.

Source of biological material Not applicable.

Statement on animal welfare Not applicable.

Conflict of interest The authors declare no competing interests.

References

- Raysyan A, Zwigart SD, Eremin SA, Schneider RJ. BPA endocrine disruptor detection at the cutting edge: FPIA and ELISA immunoassays. *Biosensors*. 2023;13(6):664.
- Michałowicz J. Bisphenol A – sources, toxicity and biotransformation. *Environ Toxicol Pharmacol*. 2014;37(2):738–58. <https://doi.org/10.1016/j.etap.2014.02.003>.
- Prueitt RL, Hixon ML, Fan T, Olgun NS, Piatos P, Zhou J, Goodman JE. Systematic review of the potential carcinogenicity of bisphenol A in humans. *Regul Toxicol Pharmacol*. 2023;142:105414. <https://doi.org/10.1016/j.yrtph.2023.105414>.
- Mukherjee U, Das S, Ghosh S, Maitra S (2024) Reproductive toxicity of bisphenol A, at environmentally relevant concentrations, on ovarian redox balance, maturational response, and intra-ocyte signalling events in *Labeo bata*. *Sci Total Environ* 906. <https://doi.org/10.1016/j.scitotenv.2023.167415>.
- Santos JDS, Pontes MDS, de Souza MB, Fernandes SY, Azevedo RA, de Arruda GJ, Santiago EF (2023) Toxicity of bisphenol A (BPA) and its analogues BPF and BPS on the free-floating macrophyte *Salvinia biloba*. *Chemosphere* 343. <https://doi.org/10.1016/j.chemosphere.2023.140235>.
- Ma Y, Liu H, Wu J, Yuan L, Wang Y, Du X, Wang R, Marwa PW, Petlulu P, Chen X. The adverse health effects of bisphenol A and related toxicity mechanisms. *Environ Res*. 2019;176:108575.
- Han E, Pan Y, Li L, Cai J (2023) Bisphenol A detection based on nano gold-doped molecular imprinting electrochemical sensor with enhanced sensitivity. *Food Chem* 426. <https://doi.org/10.1016/j.foodchem.2023.136608>.
- Liu SG, Wu T, Liang Z, Zhao Q, Gao W, Shi X (2023) A fluorescent method for bisphenol A detection based on enzymatic oxidation-mediated emission quenching of silicon nanoparticles. *Spectrochim Acta - Part A: Mol Biomol Spectrosc* 302. <https://doi.org/10.1016/j.saa.2023.123123>.
- El Hani O, Karrat A, Digua K, Amine A (2023) Advanced molecularly imprinted polymer-based paper analytical device for selective and sensitive detection of Bisphenol-A in water samples. *Microchemical Journal* 184:108157
- Zhu Y, Liang M, Liu Y, Zhong M, Zhou B, Huang L, Zhang Z. Magnetic metal-organic framework material synthesized by molecular imprinting technology for analysis of bisphenol A. *Chromatographia*. 2023;86(10):669–76. <https://doi.org/10.1007/s10337-023-04277-w>.
- Karrat A, Amine A. Solid-phase extraction combined with a spectrophotometric method for determination of bisphenol-A in water samples using magnetic molecularly imprinted polymer. *Microchem J*. 2021;168:106496. <https://doi.org/10.1016/j.microc.2021.106496>.
- Tsalbouris A, Kalogiouri NP, Kabir A, Furton KG, Samanidou VF (2021) Bisphenol A migration to alcoholic and non-alcoholic beverages – an improved molecular imprinted solid phase extraction method prior to detection with HPLC-DAD. *Microchem J* 162. <https://doi.org/10.1016/j.microc.2020.105846>.
- Wu YT, Zhang YH, Zhang M, Liu F, Wan YC, Huang Z, Ye L, Zhou Q, Shi Y, Lu B. Selective and simultaneous determination of trace bisphenol A and tebuconazole in vegetable and juice samples by membrane-based molecularly imprinted solid-phase extraction and HPLC. *Food Chem*. 2014;164:527–35. <https://doi.org/10.1016/j.foodchem.2014.05.071>.
- Yuan Y, Liu Y, Teng W, Tan J, Liang Y, Tang Y. Preparation of core-shell magnetic molecular imprinted polymer with binary monomer for the fast and selective extraction of bisphenol A from milk. *J Chromatogr A*. 2016;1462:2–7. <https://doi.org/10.1016/j.chroma.2016.06.045>.
- Chang C-M, Chou C-C, Lee M-R. Determining leaching of bisphenol A from plastic containers by solid-phase microextraction and gas chromatography–mass spectrometry. *Anal Chim Acta*. 2005;539(1–2):41–7.
- Lu J, Wu J, Stoffella PJ, Wilson PC. Analysis of bisphenol A, nonylphenol, and natural estrogens in vegetables and fruits using gas chromatography–tandem mass spectrometry. *J Agric Food Chem*. 2013;61(1):84–9.
- Maragou NC, Lampi EN, Thomaidis NS, Koupparis MA. Determination of bisphenol A in milk by solid phase extraction and liquid chromatography–mass spectrometry. *J Chromatogr A*. 2006;1129(2):165–73.
- Alenazi NA, Manthorpe JM, Lai EPC. Selective extraction of BPA in milk analysis by capillary electrophoresis using a chemically modified molecularly imprinted polymer. *Food Control*. 2015;50:778–83. <https://doi.org/10.1016/j.foodcont.2014.10.026>.
- Beduk T, Ait Lahcen A, Tashkandi N, Salama KN. One-step electrosynthesized molecularly imprinted polymer on laser scribed graphene bisphenol a sensor. *Sens Actuators, B Chem*. 2020;314:128026. <https://doi.org/10.1016/j.snb.2020.128026>.
- Jia M, Chen S, Shi T, Li C, Wang Y, Zhang H. Competitive plasmonic biomimetic enzyme-linked immunosorbent assay for sensitive detection of bisphenol A. *Food Chem*. 2021;344:128602. <https://doi.org/10.1016/j.foodchem.2020.128602>.
- Elfadil D, Lamaoui A, Della Pelle F, Amine A, Compagnone D. Molecularly imprinted polymers combined with electrochemical sensors for food contaminants analysis. *Molecules*. 2021;26(15):4607.
- Hasseb AA, Abdel Ghani NdT, Shehab OR, El Nashar RM. Application of molecularly imprinted polymers for electrochemical detection of some important biomedical markers and pathogens. *Curr Opin Electrochem*. 2022;31:100848. <https://doi.org/10.1016/j.coelec.2021.100848>.
- Liu Y-H, Liu C, Wang X-H, Li T, Zhang X. Electrochemical sensor for sensitive detection of bisphenol A based on molecularly imprinted TiO₂ with oxygen vacancy. *Biosens Bioelectron*. 2023;237:115520. <https://doi.org/10.1016/j.bios.2023.115520>.
- Han L, Zhu X, Zhang D, Liu H, Sun B. Peptide-based molecularly imprinted polymer: a visual and digital platform for specific recognition and detection of ethyl carbamate. *ACS Sensors*. 2023;8(2):694–703. <https://doi.org/10.1021/acssensors.2c02197>.
- Hassanzadeh M, Ghaemy M, Amininasab SM, Shami Z. Molecularly imprinted polymer capped near infrared fluorescent emitting Ag₂S-functionalized-COOH quantum dots for detection of creatinine as a nanosensor with high sensitivity and selectivity. *Sens Actuators, A*. 2021;331:112936. <https://doi.org/10.1016/j.sna.2021.112936>.
- Saylan Y, Erdem Ö, Inci F, Denizli A. Advances in biomimetic systems for molecular recognition and biosensing. *Biomimetics (Basel)*. 2020;5(2):20.
- Saylan Y, Denizli A. Chapter 1 - fundamentals and applications of molecularly imprinted systems. In: Denizli A, editor. *Molecular Imprinting for Nanosensors and Other Sensing Applications*. Elsevier; 2021. p. 1–17.
- Inroga FAD, Rocha MO, Lavayen V, Arguello J. Development of a tyrosinase-based biosensor for bisphenol A detection

- using gold leaf-like microstructures. *J Solid State Electrochem.* 2019;23(6):1659–66. <https://doi.org/10.1007/s10008-019-04252-2>.
29. Lu H, Xu S. Visualizing BPA by molecularly imprinted ratiometric fluorescence sensor based on dual emission nanoparticles. *Biosens Bioelectron.* 2017;92:147–53. <https://doi.org/10.1016/j.bios.2017.02.013>.
 30. Sinha A, Wu L, Lu X, Chen J, Jain R. Corrigendum to “Advances in sensing and biosensing of bisphenols: a review” [ACA 998 (2018) 1–27](S000326701731156X)(10.1016/j.aca.2017.09.048). *Anal Chim Acta.* 2018;1029:125–9. <https://doi.org/10.1016/j.aca.2018.05.047>.
 31. Wang CY, Zeng Y, Shen AG, Hu JM. A highly sensitive SERS probe for bisphenol A detection based on functionalized Au@Ag nanoparticles. *Anal Methods.* 2018;10(47):5622–8. <https://doi.org/10.1039/c8ay01966e>.
 32. Lach P, Garcia-Cruz A, Canfarotta F, Groves A, Kalecki J, Korol D, Borowicz P, Nikiforow K, Cieplak M, Kutner W, Piletsky SA, Sharma PS. Electroactive molecularly imprinted polymer nanoparticles for selective glyphosate determination. *Biosens Bioelectron.* 2023;236:115381. <https://doi.org/10.1016/j.bios.2023.115381>.
 33. Ikegami T, Mukawa T, Nariai H, Takeuchi T. Bisphenol A-recognition polymers prepared by covalent molecular imprinting. *Anal Chim Acta.* 2004;504(1):131–5. <https://doi.org/10.1016/j.aca.2003.08.032>.
 34. Goo SH, Velhal NB, Park J. Fabrication and evaluation of molecularly imprinted structured polymeric films via photopolymerization for bisphenol A detection. *MRS Commun.* 2021;11(5):576–83. <https://doi.org/10.1557/s43579-021-00077-1>.
 35. Paruli E III, Soppera O, Haupt K, Gonzato C. Photopolymerization and photostructuring of molecularly imprinted polymers. *ACS Appl Polym Mater.* 2021;3(10):4769–90. <https://doi.org/10.1021/acsapm.1c00661>.
 36. Elfadil D, Della Pelle F, Compagnone D, Amine A. Green synthesis of molecularly imprinted polymers for dispersive magnetic solid-phase extraction of erythrosine B associated with smartphone detection in food samples. *Materials.* 2022;15(21):7653.
 37. Wang J, Shen Q, Yu X, Kang Q, Shen D. A smartphone-based ratiometric fluorescence and absorbance dual-mode device for rhodamine B determination in combination with differential molecularly imprinting strategy and primary inner filter effect correction. *Microchem J.* 2022;183:108077. <https://doi.org/10.1016/j.microc.2022.108077>.
 38. Liu J, Zhan Y, Qiu B, Lin Z, Guo L. Portable smartphone platform based on aggregation-induced enhanced emission carbon dots for ratiometric quantitative sensing of fluoride ions. *ACS Sensors.* 2023;8(2):884–92. <https://doi.org/10.1021/acssensors.2c02589>.
 39. Yang T, Luo Z, Bewal T, Li L, Xu Y, Mahdi Jafari S, Lin X. When smartphone enters food safety: a review in on-site analysis for foodborne pathogens using smartphone-assisted biosensors. *Food Chem.* 2022;394:133534. <https://doi.org/10.1016/j.foodchem.2022.133534>.
 40. Palmieri S, Elfadil D, Fanti F, Della Pelle F, Sergi M, Amine A, Compagnone D. Study on molecularly imprinted polymers obtained sonochemically for the determination of aflatoxins in food. *Molecules.* 2023;28(2):703.
 41. Elfadil D, Palmieri S, Della Pelle F, Sergi M, Amine A, Compagnone D. Enzyme inhibition coupled to molecularly imprinted polymers for acetazolamide determination in biological samples. *Talanta.* 2022;240:123195.
 42. Lamaoui A, García-Guzmán JJ, Amine A, Palacios-Santander JM, Cubillana-Aguilera L (2021) Synthesis techniques of molecularly imprinted polymer composites. In: *Molecularly Imprinted Polymer Composites.* Elsevier, pp 49–91.
 43. Elfadil D, Saidi K, Amine A. Selective extraction of maleic hydrazide in foods using magnetic molecularly imprinted polymers and colorimetric detection via smartphone. *Talanta.* 2024;269:125488.
 44. Fuchs Y, Soppera O, Haupt K. Photopolymerization and photostructuring of molecularly imprinted polymers for sensor applications—a review. *Anal Chim Acta.* 2012;717:7–20. <https://doi.org/10.1016/j.aca.2011.12.026>.
 45. Gallo P, Di Marco PI, Esposito F, Fasano E, Scognamiglio G, Mita GD, Cirillo T. Determination of BPA, BPB, BPF, BADGE and BFDGE in canned energy drinks by molecularly imprinted polymer cleaning up and UPLC with fluorescence detection. *Food Chem.* 2017;220:406–12. <https://doi.org/10.1016/j.foodchem.2016.10.005>.
 46. Li J, Zhou H, Liu Y-X, Yan X-Y, Xu Y-P, Liu S-M. Solid-phase extraction for selective determination of bisphenol A in drinks and fruits by dummy surface molecularly imprinted polymer with direct synthetic method. *Food Addit Contam: Part A.* 2014;31(6):1139–46. <https://doi.org/10.1080/19440049.2014.906751>.
 47. Huang X-C, Ma J-K, Wei S-L. Preparation and application of a novel magnetic molecularly imprinted polymer for simultaneous and rapid determination of three trace endocrine disrupting chemicals in lake water and milk samples. *Anal Bioanal Chem.* 2020;412(8):1835–46. <https://doi.org/10.1007/s00216-020-02431-z>.
 48. Bhogal S, Mohiuddin I, Kaur K, Lee J, Brown RJC, Malik AK, Kim K-H. Dual-template magnetic molecularly imprinted polymer-based sorbent for simultaneous and selective detection of phenolic endocrine disrupting compounds in foodstuffs. *Environ Pollut.* 2021;275:116613. <https://doi.org/10.1016/j.envpol.2021.116613>.

Publisher's Note Springer Nature remains neutral with regard to jurisdictional claims in published maps and institutional affiliations.

Springer Nature or its licensor (e.g. a society or other partner) holds exclusive rights to this article under a publishing agreement with the author(s) or other rightsholder(s); author self-archiving of the accepted manuscript version of this article is solely governed by the terms of such publishing agreement and applicable law.